

## Biomathematical Modeling Approach to Predict Clinical SUVRs for Amyloid PET Imaging

著者	Shidahara M., Seki C., Nai YH., Okamura N., Furumoto S., Yanai K., Watabe H., Tashiro M.
journal or publication title	CYRIC annual report
volume	2016-2017
page range	147-151
year	2017
URL	<a href="http://hdl.handle.net/10097/00128081">http://hdl.handle.net/10097/00128081</a>

## VII. 5. Biomathematical Modeling Approach to Predict Clinical SUVs for Amyloid PET Imaging

Shidahara M.<sup>1,2</sup>, Seki C.<sup>3</sup>, Nai YH.<sup>2</sup>, Okamura N.<sup>4</sup>, Furumoto S.<sup>2</sup>,  
Yanai K.<sup>5</sup>, Watabe H.<sup>2</sup>, and Tashiro M.<sup>2</sup>

<sup>1</sup>Department of Quantum Science and Energy Engineering, Tohoku University

<sup>2</sup>Cyclotron Radioisotope Center, Tohoku University

<sup>3</sup>National Institutes for Quantum and Radiological Science and Technology

<sup>4</sup>Faculty of Medicine, Tohoku Medical and Pharmaceutical University

<sup>5</sup>Department of Pharmacology, Tohoku University School of Medicine

### Introduction

The aggregation of amyloid  $\beta$  peptide is one of the pathological observations in the brains of individuals with Alzheimer's disease (AD). Amyloid imaging using positron emission tomography (PET) has been recognized as having an important role in the diagnosis of AD<sup>1</sup>). In the last decade, many PET radioligands for amyloid imaging have been developed; some of them have successfully been applied in human PET studies.

In general, the discovery and development of radioligands for clinical application requires complicated and sometimes empirical procedures in terms of chemical (e.g., stability of labeling and lipophilicity) or biological (e.g., affinity, metabolites and density of the target) factors<sup>2,3</sup>). Even though these factors have been well-investigated in the case of candidate radioligands, several factors obtained in *in vitro* or *in vivo* animal studies may not be applicable to human studies; it is not easy to develop successful radioligands and satisfy clinical demands<sup>4</sup>). We need to know not only the micro parameters of the candidate radioligands but also overall macroscopic performance.

Recently, there has been growing interest concerning more efficient development of successful radioligands in clinical studies using systematic evaluation of their overall performance (e.g., outcome measures)<sup>3</sup>). It is obvious that the use of *in vivo* PET scans in experimental animals or humans is the fastest and easiest approach for the evaluation of the overall performance of the candidate radioligand. However, the development of a labelling protocol for positron emitter isotopes and the synthesis of a radioligand for PET studies are

labor intensive and also take considerable time. Therefore, in order to contribute on the radioligand development, we proposed a new method to predict standardized uptake value (*SUVR*) of amyloid PET radioligands using biomathematical modeling and *in silico* parameters (Fig. 1)<sup>5</sup>. The methodology includes empirical formula of lipophilicity ( $\log P$ ), free fraction of radioligand in blood ( $f_p$ ) and free fraction of radioligand in tissue ( $f_{ND}$ ). In this study, we investigated the influence of empirical formulae based on 3 datasets of  $f_p$  and  $f_{ND}$  reported by Guo et al.<sup>3</sup>, Summerfield et al.<sup>6</sup>, and Wan&Mauer<sup>7,8</sup> on the outcome, predicted *SUVRs*, of [<sup>11</sup>C]PiB, [<sup>11</sup>C]BF-227, [<sup>11</sup>C]AZD2184, [<sup>11</sup>C]SB-13, [<sup>18</sup>F]FACT, [<sup>18</sup>F]florbetapir, [<sup>18</sup>F]florbetaben, [<sup>18</sup>F]flutemetamol, [<sup>18</sup>F]FDDNP and [<sup>18</sup>F]AZD4694.

## Material and Methods

We assumed that the radioligand for amyloid imaging obeyed the simplified one-tissue compartment model (1TCM) (Fig. 1). The kinetic parameters ( $K_1$ ,  $k_2$  and  $BP_{ND}$ ) for each radioligand in the human brain were mathematically modelled, where  $K_1$ ,  $k_2$  and  $BP_{ND}$  are the influx and efflux rate constants between arterial plasma and brain tissue, and the binding potential, respectively. The time–activity curves (TACs), with or without specific binding of the radioligand in brain tissue, were calculated as follows:

$$\begin{aligned} C_{target}(t) &= K_1 \cdot C_p(t) \otimes \exp\left[-\left(\frac{k_2}{1 + BP_{ND}}\right)t\right] \\ C_{reference}(t) &= K_1 \cdot C_p(t) \otimes \exp(-k_2 t) \end{aligned} \quad (1)$$

where  $C_{target}$  is the TAC of the target region, where the radioligand specifically binds to the target protein.  $C_{reference}$  is the TAC of the reference region without the target protein.  $C_p$  is the arterial plasma input function. The influx rate constant from plasma to brain tissue,  $K_1$  [mL/cm<sup>3</sup>/min] was formulated using the Renkin–Crone model as follows:

$$K_1 = f \cdot \left[1 - e^{(-PS/f)}\right] \quad (2)$$

where  $P$ ,  $f$  and  $S$  are capillary permeability [cm/min], perfusion [mL/cm<sup>3</sup>/min] and capillary surface area [cm<sup>2</sup>/cm<sup>3</sup> of brain], respectively.  $f$  and  $S$  were set to 0.6 [mL/cm<sup>3</sup>/min] and 150 [cm<sup>2</sup>/cm<sup>3</sup> of brain], respectively. Permeability  $P$  in **Eq. (2)** was empirically formulated as follows<sup>3</sup>:

$$P = 10^{\{-0.121(c \log D - 2.298)^2 - 2.544 \log(V_x^{1/3}) - 2.525\}} \quad (3)$$

where  $c \log D$  and  $V_x$  are lipophilicity and the McGowan volume [cm<sup>3</sup>/mol/100], respectively. The efflux rate constant from brain tissue to plasma,  $k_2$  [1/min], was expressed using the following equation, assuming equilibrium in the radioligand

concentrations between plasma and brain tissue.

$$k_2 = \frac{V_{aq\_P} \cdot K_1}{V_{aq\_T}} \cdot \frac{f_{ND}}{f_P} \quad (4)$$

where  $V_{aq\_P}$  and  $V_{aq\_T}$  are the apparent aqueous volume in plasma, the apparent aqueous volume in tissue and these were set to 0.98 [solvent/mL of plasma] and 0.9 [solvent/mL of tissue], respectively<sup>3)</sup>. Both  $f_P$  and  $f_{ND}$  were estimated from empirical formulae, which were established from  $f_P$  and  $f_{ND}$  measured from *in vitro* binding experiments using mouse brain and plasma, and *in silico* lipophilicity. Here in this study, we tested 3 data sets of  $f_P$  and  $f_{ND}$  reported by Guo et al.<sup>3)</sup>, Summerfield et al.<sup>6)</sup>, and Wan&Mauer<sup>7,8)</sup>. The radioligand binding capacity at the target site,  $BP_{ND}$ , was modelled<sup>5)</sup> as follows:

$$BP_{ND} = f_{ND} \left\{ \frac{B_{avail-42}}{K_{D-42}} + \frac{B_{avail-40}}{K_{D-40}} \right\} = f_{ND} \left\{ \frac{a}{K_{D-42}} + \frac{(1-a)}{K_{D-40}} \right\} B_{avail} \quad (5)$$

$$B_{avail} = B_{avail-42} + B_{avail-40}$$

where  $a$ ,  $K_{D-42}$  and  $K_{D-40}$  are the fractions of  $A\beta_{1-42}$ , the dissociation constant for  $A\beta_{1-42}$  and  $A\beta_{1-40}$ , respectively.  $B_{avail-42}$ ,  $B_{avail-40}$  and  $B_{avail}$  were available binding sites of  $A\beta_{1-42}$  and  $A\beta_{1-40}$ , ( $A\beta_{1-42} + A\beta_{1-40}$ ), respectively.  $a$  was assumed to have a value of 0.7, which is biochemically derived from fractions of extra-cellular insoluble  $A\beta_{1-42}$  in both AD and HC brains<sup>9)</sup>. The TACs of the target and reference regions were calculated using  $K_1$ ,  $k_2$  and  $BP_{ND}$  and fixed arterial input function  $C_p$  using Eq. (1). The parameter of interest,  $SUVR$ , was then estimated from the predicted TACs. Finally, for each data sets of  $f_P$  and  $f_{ND}$ , the predicted  $SUVR$  were compared with their clinical counterparts,  $SUVR$ <sup>5)</sup>.

## Results and discussion

Figure 2A shows the relationships between *in silico* lipophilicity and *in vitro*  $f_{ND}$ , and Fig. 2B shows the relationships between *in vitro*  $f_{ND}$  and  $f_P$  using the datasets of Guo's, Summerfield's and Wan&Maurer's, respectively. For each dataset, correlations between lipophilicity and  $f_{ND}$  and between  $f_{ND}$  and  $f_P$  were observed. Figure 3 shows the relationship between predicted  $SUVR$  and clinically observed  $SUVR$ s, these results were obtained by applying empirical formulae in Fig. 2 into the prediction scheme of  $SUVR$  of the 10 amyloid radioligands. In this study, we calculated Moriguchi logP as the lipophilicity<sup>5)</sup>. Even though there was inconsistent use of lipophilicity between the 3 datasets (clogD and clogP by different softwares) and ours ( $MlogP$ ) for the estimation of  $f_P$  and  $f_{ND}$ , positive

correlations between predicted and clinically observed SUVRs were observed (Fig. 3). These results supported the fact that our approach (*MlogP*) without the use of *in vitro* experiments for  $f_p$  and  $f_{ND}$  estimation can be applied to other amyloid radioligands, even though the data-sets selected for estimation of  $f_p$  and  $f_{ND}$  resulted in different values of the predicted SUVRs.

## Conclusion

For all 3 data sets of  $f_p$  and  $f_{ND}$ , predicted *SUVR* showed good correlation with clinically observed *SUVR* for the 10 clinically applied amyloid tracers, however, the values of predicted *SUVR* were different from each datasets. These results will be contributed on the future improvement of the methodology.

## References

- 1) Okamura N, Harada R, et al. *Ageing Res Rev.* (2016) 107-13.
- 2) Innis RB, Cunningham VJ, et al. *J Cereb Blood Flow Metab.* **27** (2007) 1533-9.
- 3) Guo Q, Brady M, et al. *J Nucl Med.* **50** (2009) 1715-23.
- 4) Laruelle M, Slifstein M, et al. *Mol Imaging Biol.* **5** (2003) 363-75.
- 5) Arakawa Y, Nai Y, et al. *J Nucl Med.* **58** (2017) 1285-92.
- 6) Summerfield SG, Read K, et al. *J Pharmacol Exp Ther.* **322** (2007) 205-13.
- 7) Maurer TS, Debartolo DB, et al. *Drug metabolism and disposition: the biological fate of chemicals.* **33** (2005) 175-81.
- 8) Wan H, Rehgren M, et al. *J Med Chem.* **50** (2007) 4606-15.
- 9) Steinerman JR, Irizarry M, et al. *Arch Neurol.* **65** (2008) 906-12.

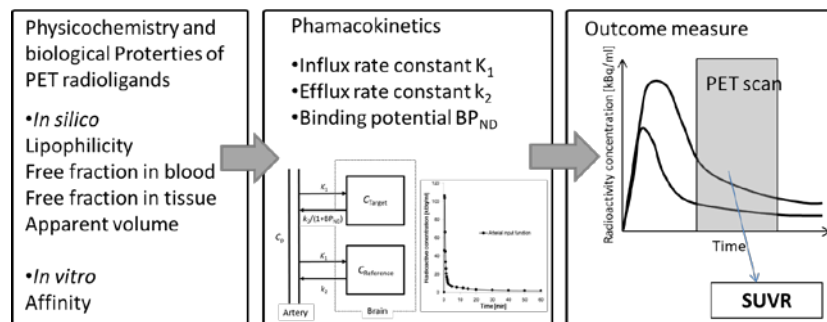


Figure 1. Overview of our biomathematical model: From physicochemical/biological properties of PET radioligand, pharmacokinetic parameters ( $K_1$ ,  $k_2$  and  $BP_{ND}$ ) are estimated, then outcome measure (*SUVR*) is predicted through time activity curves of simplified 1 tissue model for both target and reference regions.

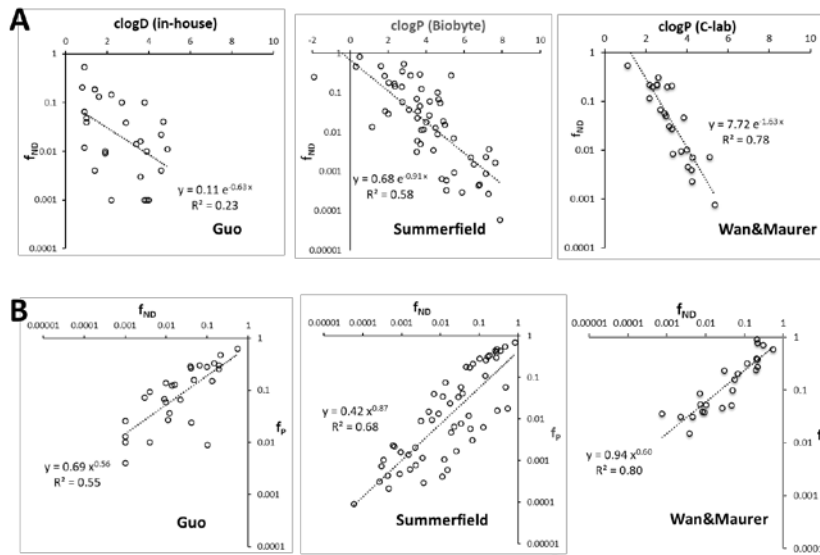


Figure 2 Relationship between in silico lipophilicity and  $f_p$  (A) and between  $f_p$  and  $f_{ND}$  (B) for 3 databases of Guo's, Summerfield's and Wan&Maurer's.

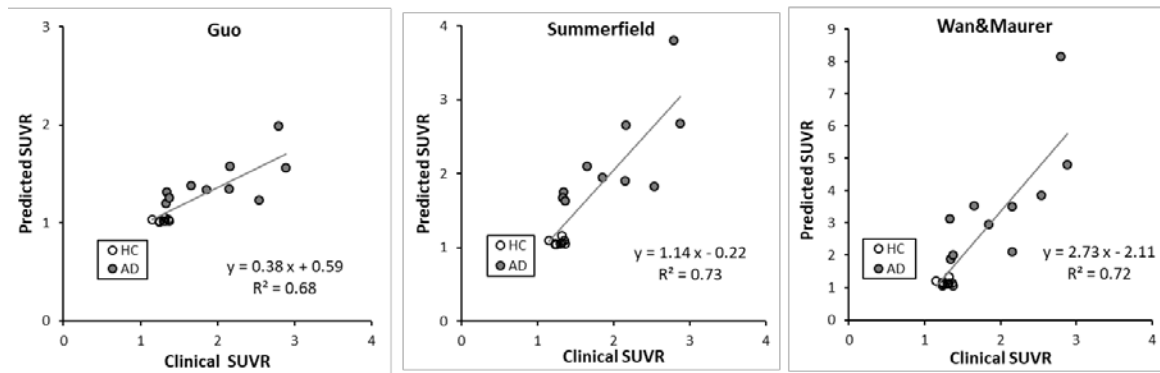


Figure 3 Relationship between clinically observed SUVR and predicted SUVR by our model based on 3 databases, Guo's (A), Summerfield's (B) and Wan&Maurer's (C).